Surface D2 Autoreceptor Expression on Substantia Nigra Dopamine Neuron Dendrites

John T Williams (williamj@ohsu.edu)
Oregon Health & Science University https://orcid.org/0000-0002-0647-6144

Joseph J. Lebowitz
Oregon Health & Science University

James R. Bunzow
Oregon Health & Science University

Brooks Robinson
Oregon Health & Science University

Susan R. Sesack
Pitt: University of Pittsburgh

Research Article

Keywords: D2 receptor, dopamine, substantia nigra, dendrodendritic, autoreceptor

Posted Date: April 28th, 2021

DOI: https://doi.org/10.21203/rs.3.rs-435162/v1

Abstract

G-Protein coupled D2 receptors expressed on dopamine neurons, i.e. D2-autoreceptors (D2Rs), negatively regulate transmitter release and cell firing in axonal terminals and somatodendritic compartments. However, as the membrane distribution of D2Rs at somatodendritic signaling sites has not been fully characterized, functional mechanistic details remain uncertain. This study utilized a knockin mouse to examine surface D2Rs linked at the N-terminus to a superecliptic pHlourin green fluorescent protein epitope (SEP) in dopamine neurons of the substantia nigra. By incubating live slices with a highly specific anti-SEP antibody, the selective labeling of plasma membrane associated receptors was achieved. The SEP-D2Rs appeared as puncta like structures apposed to the surface of dendrites and soma of dopamine neurons. The percentage of D2R expression apposed to TH positive structures varied linearly with the density of TH fibers observed. TH-associated SEP-D2Rs displayed a cell surface density of 0.180 puncta per μm^2, which corresponds to an average frequency of 1 punctum every 1.326 μm using nearest neighbor analysis. The distinct punctate appearance of the anti-SEP staining indicates there is a population of D2Rs organized in discrete clusters along the plasma membrane, an arrangement that can spatially localize signaling and influence GPCR efficacy. The results also indicate that D2Rs are spatially distributed on the plasma membrane at a frequency higher than previously reported.

Introduction

Midbrain to forebrain dopamine transmission regulates locomotion, cognition, motivation, and affective states (Beeler and Dreyer, 2019; Berke, 2018). Human pathologies involving dopamine signaling are diverse and include movement (Parkinson's Disease) and mental (schizophrenia, ADHD) disorders (Grace, 2016; Hirsch et al., 1988; Tripp and Wickens, 2009). Furthermore, the actions of drugs of abuse on dopamine neurons contribute to addiction, while therapeutic ligands modulating dopamine signaling are used clinically to treat these various disorders (e.g. amphetamine, haloperidol) (Koob and Volkow, 2016; Pontieri et al., 1995). A key regulator of dopamine transmission is the D2 autoreceptor (D2R) expressed on dopamine neurons. D2Rs typify the D2-like dopamine receptor family (including D3R, D4R) by coupling to G_i/G_o proteins to decrease cAMP (via inhibition of adenylate cyclase) and leading to downstream effects by decreasing phosphorylation of PKA (protein kinase A) (Beaulieu and Gainetdinov, 2011). D2Rs also signal through functional interactions with ion channels, inhibiting voltage gated calcium channels and activating G-protein activated inwardly rectifying potassium channels (GIRKs) to pause neuronal firing and inhibit dopamine release at terminals and somatodendritic compartments (Beckstead et al., 2004; Ford, 2014). A mutation in the gene encoding D2Rs was recently linked to a hyperkinetic movement disorder in humans, while *in vitro* disruptions in D2R expression have been shown to dysregulate neuronal complexity and viability (Giguère et al., 2019; Weijden et al., 2020).

Dopamine neurons alternate between tonic pacemaker activity and phasic burst firing, and these patterns are regulated by multiple mechanisms (Grace and Bunney, 1983). Dopaminergic action potentials originate at axon initial segments that often arise from proximal dendrites and are then backpropagated through the soma and dendrites from where dopamine release can be triggered (González-Cabrera et al.,

2017; Grace and Bunney, 1983). Previous work has shown that D2Rs gate action potential backpropagation in dendritic compartments (Gentet and Williams, 2007). However, knowledge gaps about the frequency and localization of dendritic D2R signaling sites continue to prevent a full understanding of neurotransmission in the dendrites of dopamine cells. Studies using electron microscopy suggest that in the substantia nigra pars compacta (SNc) D2R expression at the plasma membrane is sparse and specialized dendro-dendritic synapses are infrequent (Groves and Linder, 1983; Sesack et al., 1994).

This study utilized a knockin mouse expressing a SEP epitope on the N-terminus of the endogenous D2R and sub-diffraction limited microscopy to localize surface D2Rs in the SNc. The results show that D2Rs are expressed in punctate structures in a relatively uniform density on the plasma membrane of the soma and dendrites of SNc dopamine neurons. The unusual spatial topology and density of expression has implications for better understanding dopamine autoregulation in this region. In a companion paper (Trinkle et al., 2021), the knockin mice were used for further subcellular exploration of D2R localization in this region.

Methods

Animal housing and generation of SEP tagged D2R knockin mice.

A detailed description of the generation of the SEP tagged D2R knockin mice was published previously (Robinson et al., 2017). Briefly, a SEP was fused to the amino terminus of the mouse D2R. This was then targeted via a knockin vector to ultimately generate SEP-D2R mice on a C57/BL6J background. Mice were maintained at the OHSU mouse facility on a standard light/dark cycle. Homozygote animals were viable and required no special care. They bred normally and so could be used for further breeding. Wild-type C57/BL6J mice were used for control experiments where noted. All protocols and procedures were approved by and followed the policies of the Oregon Health and Science University IACUC.

Slice Preparation and live SEP-D2R Staining

Mice were anesthetized with isoflourane before rapid decapitation and brain removal into Krebs-Ringer solution containing (in mM): 126 NaCl, 1.2 MgCl2, 2.4 CaCl2, 1.4 NaH2PO4MK-801 (10 µM). Horizontal midbrain sections of 220 µm were cut using a vibratome in warmed (35°C) Krebs. Slices were allowed to recover in warm Krebs bubbled with 95% O_2/5%CO_2 in MK-801 (10 µM) for 30 minutes to allow the slices to recover.

Live slices were incubated in a rabbit polyclonal anti-GFP antibody Alexa Flour 488 conjugated (Life Technologies A21311) at 1:400 dilution in 2-3 mL Krebs for 1 hr, then washed for 15 min in fresh Krebs. Slices were fixed with 4% paraformaldehyde (PFA) in phosphate-buffered saline (PBS) for 30 min at room temperature. Slices were blocked and permeabilized for 1 hr at RT in PBS + 0.5% fish skin gelatin (FSG) + 0.5% Tween 20. A primary antibody was then applied overnight at 4ºC to label tyrosine hydroxylase (TH) (Mouse monoclonal Sigma T-1299) at a 1:500 dilution in PBS+0.5% FSG. After washing in RT PBS 3

times for 15 min each, the appropriate secondary antibodies (Thermo Fisher) were incubated at RT at a 1:500 dilution in PBS+0.5% FSG. Neurons filled with Neurobiotin were incubated with streptavidin conjugated to Alexa Fluor 594 during the initial block and permeabilization (1:1000 Thermo Fisher S11226) with all subsequent steps identical to non-filled cells. Sections were mounted using Fluoromount (Sigma) and sealed with nail polish. Concerns about the anti-GFP antibody crosslinking the SEP-D2Rs to cause clustering were addressed by using a nanobody to GFP in 2P imaging or prefixing the slice for 10 minutes in PBS+4% PFA at RT and then staining with the anti-GFP 488 in PBS with no detergent present after which the punctate staining pattern of the anti-GFP antibody was still seen (Robinson et al., 2017).

Imaging of sections by CLSM

Images were acquired on a either a Zeiss 880 confocal system with Fast Airyscan, or a Zeiss 980 confocal system with Airyscan2-multiplex. Each Airyscan image contains positional information that enables the reconstruction of a single sub-diffraction image at a resolution of 140 nm in the lateral X/Y axis and 400 nm in the Z axis. Channels were imaged in non-overlapping sequence and captured as a z-stack using Zen software (Zeiss). Airyscan2 determines a calculated laser output derived from a modified beam, and by this measure, no more than 5% of maximum laser power was used to acquire images. Because antibody penetration is limited to 5-10 µm in the fixed slices, images were collected below the cut surface usually starting at a depth of ~1 µm and collected as Z stacks (3 µm total depth) sectioned at a 150 nm step size. For images of Neurobiotin filled cells, the upper and lower z boundaries were set to capture the entire field of visible processes of the single cell.

Inclusion criteria for SEP-D2R puncta

The minimum diameter (X/Y) and depth (Z) of defined puncta were set according to Nyquist sampling criteria of the known pixel and voxel sizes (280nm for x/y, 800nm for z) and were detected according to the point spread function for diffracted light. These parameters were used for automated 3D identification and analysis of individual D2R puncta using the “spots” function in IMARIS 9.6. Identified puncta were secondarily subjected to a quality filter within the IMARIS spots algorithm (minimum quality – 300) to ensure that each spot represented a labeled receptor and was not influenced by background noise. This criterion likely underestimates the number of puncta but increases confidence that the staining is specific to surface SEP-D2Rs.

Surface D2R density in SNc dopamine neurons

Using the surfaces function, an approximate volume was created for TH-stained dendrites resulting in a 3D binary mask representing their position in space. TH is a highly expressed intracellular marker in dopamine neurons allowing for a reasonable estimation of plasma membrane boundaries and morphology. Spots were identified and populated into the 3D image as described above. To specifically examine D2Rs on dopamine cells, a filter was applied to select spots whose center was ≤250 nm to the TH surface. These TH apposed puncta were included for all density and localization analyses. Any

puncta ≥250 nm from a TH(+) surface were presumed to be surface receptors on non-dopaminergic cell types, as all receptors express the SEP epitope.

Results

Cell Surface Staining of D2Rs on dopamine neurons in the SNc

Images of the SEP-D2Rs in the SNc following incubation of live slices with the anti-GFP Alexa 488 showed numerous discrete puncta associated with TH positive processes as well as less frequent puncta not apposed to TH stained processes **(Figures 1-3)**. Fluorescent puncta not apposed to TH labeled dendrites were presumed to be receptors on non-dopaminergic structures such as afferent terminals. The anti-GFP polyclonal antibody used is linked with 6-8 Alexa Flour 488 fluorophores such that the signal is highly amplified. When the SEP-D2R stained puncta were imaged at high power, they were markedly discrete in the X/Y plane and had a characteristic ovoid appearance in Z stacks **(Figure 1C)**. On average, the diameter of manually selected puncta was ~250-500 μm, or at the limit of resolution of our system **(Figure 1C)**. The intensity of selected puncta measured using intensity summation of all the voxels contained within a spot was variable. Experiments using wild type animals detected a total of 34,271 fluorescent puncta with a maximum intensity of 12,799 arbitrary units (AUs) and a minimum of 212 AUs. Conversely, a total of 12,855 puncta from SEP-D2R knockin animals had an intensity range of 456,725 to 1,135 AUs (data not shown). These semi-quantitative observations led us to conclude that SEP-D2Rs are organized in a variable but unknown number of receptors tightly packed in discrete membrane-bound clusters. Given the difference in intensities of puncta between knockin and wild type animals, further selection of puncta in 3D was done in an unbiased manner using the IMARIS “spots quality” algorithm.

In order to rule out intrinsic fluorescence from the SEP epitope as contributing to the measured puncta signals, 1-2 slices from 2 animals were incubated without the anti-GFP488 and imaged under identical settings as anti-SEP labeled slices. As the spot quality threshold utilizes an absolute and not a relative value to determine threshold, the value of 300 was used across groups. Comparing the number of puncta detected in labeled slices vs. those without primary antibody confirmed both that the amount of intrinsic SEP fluorescence in brain slices is negligible and the puncta being detected in labeled slices are truly labeled surface D2Rs (**figure 2 A,B; table 1).** To further confirm that SEP signal was not influencing data more subtly than the spot detection algorithm can reveal, the intensities from the brightest 40% of puncta in labeled and unlabeled slices were compared and corroborated the identity of labeled D2R puncta.

Surface distribution of SEP-D2Rs

In order to study the 3D distribution of SEP-D2Rs on the dendrites of dopamine cells, individual puncta were identified using the “spots” function and an automated detection pipeline in the IMARIS imaging software. Each spot in this analysis represented a point in 3D space identified as a discrete object using a custom quality filter intrinsic to the IMARIS “spots” algorithm. The density of spots associated with TH(+) dendrites averaged 0.180 puncta/μm^2 with an average nearest neighbor distance of 1.326 μm between

two spots. On average, 44.6% of spots were apposed to TH rendered surfaces, and the remaining spots were not associated with areas of TH staining (**figure 2C**, **table 1**). The former value varied between fields of view, ranging from 26.75 to 65.84%, likely reflecting the relative density of TH-positive dendrites. Indeed, the percentage of SEP-D2Rs apposed to TH dendrites showed a significant positive correlation with the fraction of the image volume occupied by TH as determined by the surfaces function in IMARIS (**figure 2D**, R^2 =0.5503, p = 0.0057). Of note, this analysis was restricted to discrete puncta apposed to the surface of TH stained processes, as these puncta likely represent clusters of D2Rs along the dendritic portion of dopamine neurons. It is possible a diffusely distributed pool of D2Rs along the cell surface was not detected due either to a relatively weak signal compared to clustered receptors, or non-distinction as a discrete object by the spots algorithm.

D2Rs are expressed at TH(+) intersections distal from the cell body

The data presented thus far establish the density of D2Rs that likely act as autoreceptors in dopamine dendrites in regions of the SNc where dendritic processes are extensive. However, because of the large and complex anatomy of dopamine cells, it is difficult to know when two crossing dendrites are from one or distinct neurons. To this end, we performed surface labeling on slices that had individual cells filled with Neurobiotin using a patch pipette. Examination of Neurobiotin filled cells confirmed that D2R puncta were observed at TH(+) membrane intersections of distinct dopamine neurons (**figure 3**). These SEP-D2R containing intersections were observed hundreds of μm's away from the soma, suggesting that dopamine neurons signal at D2R sites distal from the soma and axon initial segments where AP's are generated (**figure 3b**). Future work will be required to determine the relative functionality of receptor sites associated with presynaptic release sites at varying distances along proximal and distal dendrites.

Discussion

The present study used a knockin animal that expressed a SEP-D2R to examine the distribution of D2Rs along the dendrites of SNc dopamine neurons. With the methods used, only receptors present on the plasma membrane were stained. The relative percentage of D2Rs associated with TH positive neurons tracked with the density of fibers, and therefore autoreceptors are likely to represent a majority of the D2Rs present in areas of high dendritic density. Despite that, the presence of D2Rs on non-TH(+) structures, likely axon terminals, suggests that D2R's can regulate afferent input signals to SNc dendrites (Trinkle et. al. 2021). Although the presence of D2Rs on dopamine neurons has been known for decades, the distribution of plasma membrane receptors examined over a wide area of SNc dendrites has not previously been determined with such precision.

The punctate distribution of the epitope tagged D2Rs on the cell surface of SNc dopamine neurons has been described previously (Gantz et al., 2015; Robinson et al., 2017). Additionally, the SEP-D2Rs in the knockin mouse are functional, and the characteristics of the D2R-evoked IPSC are similar to those in the wild type mouse(Robinson et al., 2017). However, it was shown that the SEP-D2Rs are expressed at a level roughly half that seen in wild-type animals. Comparing earlier work that also revealed a punctate

distribution of FLAG epitope tagged D2Rs expressed at ~150% of wild-type levels, we hypothesize that the distribution of receptors into discrete puncta is tightly regulated and not sensitive to receptor expression levels (Gantz et al., 2015; Robinson et al., 2017). T. Using an antibody highly specific to an extracellular epitope attached to the knockin SEP-D2R, we overcame technical barriers surrounding antibody specificity to GPCRs that have prevented complete characterizations of the distribution of endogenous D2Rs. It is possible that fluorescent ligands capable of labeling D2Rs with high specificity may ultimately overcome remaining limitations (Arttamangkul et al., 2019; Guthrie et al., 2020). However, given the punctate distribution observed in two distinct transgenic lines with differing levels of expression and epitope tags, it can be assumed that endogenous receptors are organized into a similar distribution. Indeed, comparable observations from EM in the companion paper (Trinkle et al., 2021) support this assumption.

Live surface staining has previously been used in noradrenergic neurons taken from a transgenic mouse expressing an amino terminus Flag tagged mu opioid receptor (MOR). The cellular distribution of MORs was diffuse along the perimeter of the cell body and dendrites in a uniform staining pattern (Arttamangkul et al., 2008). A similar approach was used to visualize the cell surface expression of the dopamine transporter (DAT) in midbrain slices of a knockin hemagglutinin virus (HA) epitope tagged DAT. Cell surface staining of the HA-DAT detected a homogenous diffuse staining in dendrites of the SNc, which contrasts to the discrete punctate appearance of D2Rs in the SEP-D2R knockin mouse (Block et al., 2015). Interestingly, when FLAG-tagged D2Rs were expressed under control of the TH promoter in the locus coeruleus (LC), staining for the FLAG tag appeared diffuse along the cell surface of LC neurons and not punctate (Robinson et al., 2017). This suggests that the organization of D2Rs into puncta as seen in SNc dendrites is cell type specific, even when compared to similar neuromodulatory neuronal environments. Recent work has revealed that organization into receptor clusters can enhance the signaling efficacy of GPCRs with downstream components like GIRK channels (Touhara and MacKinnon, 2018). Dopamine neurons have repeatedly been shown to function under large energetic burdens that render them vulnerable to cellular insults and aging (Bolam and Pissadaki, 2012; Guzman et al., 2010; Pacelli et al., 2015; Surmeier et al., 2017). It is possible that dopamine cells have conserved the organization of D2Rs into puncta to compensate for this energetic stress. Supporting this hypothesis is recent work showing an enhancement of neuronal arborization and concomitant increase in cellular vulnerability in response to D2R deletion in dopamine neurons (Giguère et al., 2019). However, determining the regulatory mechanisms that control the assembly of D2Rs into puncta and how these D2Rs are organized at the plasma membrane will require further experimentation.

An important consideration is how to reconcile our immunofluorescence staining demonstrating a high level of expression of the SEP-D2R on the cell surface of dopamine neurons with EM studies showing sparse extrasynaptic labeling of D2Rs in dopamine cells (Sesack et al., 1994; Uchigashima et al., 2016; Yung et al., 1995) (see also Trinkle et al., 2021). Most probably, D2R puncta on the dendrites of SNc dopamine neurons are sensitive to the strong fixation processes and limited antibody penetration issues inherent to traditional EM techniques. $GABA_A$ receptor subunits have previously been shown to display

either a uniform or punctate distribution depending on whether receptors were labeled in perfused animals (uniform) or lightly fixed acute or frozen sections (punctate)(Schneider Gasser et al., 2006). Live cell staining allows for the antibody to diffuse through the extracellular space (ECS) which is ~30% of the total volume of the SNc, whereas fixation has been shown to decrease extracellular volume (Cragg et al., 2001; Hrabetova et al., 2018). Additionally, even serially-collected EM images representing a 3D structure can typically only sample dimensions on the order of single microns, whereas fluorescent labeling and imaging allows for the measurement of D2Rs along 10's of microns of neuronal processes. With that said, an important caveat of this work is that we only investigated the density of D2Rs in 3D-space associated with TH membranes. We do not know the degree to which each postsynaptic receptor cluster is associated with a presynaptic release site. Future work will aim to determine the spatial frequency of D2Rs lying adjacent to sites of dendritic dopamine release.

Declarations

Acknowledgements: This work was supported by National Institutes of Health Grants DA004523 and DA007262 (Williams). We acknowledge expert technical assistance by staff in the Advanced Light Microscopy Core, supported by grant P30NS061800.

Funding

DA004523 and DA007262 (Williams)

Conflicts of interest/Competing interests

None of the authors report a conflict of interest. One author (SRS) acknowledges being a Co-Editor-In-Chief of this journal.

Availability of data material

The datasets generated and/or analyzed during the current study are available from the corresponding author at reasonable request.

Code availability

Not applicable.

Authors' contributions

J.R.B. created the superecliptic pHluorin-tagged D2 receptor knockin mouse. J.R.B., S.R.S., and J.T.W. designed the studies. J.J.L., J.R.B., and B.R. performed and analyzed the live labeling and imaging experiments. The paper was written by J.J.L and J.R.B with editorial contributions from S.R.S and J.T.W. All authors read and approved the final manuscript.

Ethics Approval

All animal procedures and protocols were conducted in accordance with the National Institute of Health *Guidelines for the Care and Use of Laboratory Animals*. They also complied with the appropriate guidelines set forth by the Institutional Animal Care and Use Committees at Oregon Health & Science University.

Consent to participate

Not applicable.

Consent to publication

All authors acknowledge participation in the study and development of the manuscript. All authors acknowledge reading the submitted form of this paper and consent to its submission for publication at this time.

References

1. Arttamangkul S, Plazek A, Platt EJ, Jin H, Murray TF, Birdsong WT, Rice KC, Farrens DL, Williams JT (2019) Visualizing endogenous opioid receptors in living neurons using ligand-directed chemistry. eLife 8:e49319. https://doi.org/10.7554/eLife.49319
2. Arttamangkul S, Quillinan N, Low MJ, Zastrow M von, Pintar J, Williams JT (2008) Differential Activation and Trafficking of μ-Opioid Receptors in Brain Slices. Mol Pharmacol 74:972–979. https://doi.org/10.1124/mol.108.048512
3. Beaulieu J-M, Gainetdinov RR (2011) The Physiology, Signaling, and Pharmacology of Dopamine Receptors. Pharmacol Rev 63:182–217. https://doi.org/10.1124/pr.110.002642
4. Beckstead MJ, Grandy DK, Wickman K, Williams JT (2004) Vesicular Dopamine Release Elicits an Inhibitory Postsynaptic Current in Midbrain Dopamine Neurons. Neuron 42:939–946. https://doi.org/10.1016/j.neuron.2004.05.019
5. Beeler JA, Dreyer JK (2019) Synchronicity: The Role of Midbrain Dopamine in Whole-Brain Coordination. eNeuro 6. https://doi.org/10.1523/ENEURO.0345-18.2019
6. Berke JD (2018) What does dopamine mean? Nat Neurosci 21:787–793. https://doi.org/10.1038/s41593-018-0152-y
7. Block ER, Nuttle J, Balcita-Pedicino JJ, Caltagarone J, Watkins SC, Sesack SR, Sorkin A (2015) Brain Region-Specific Trafficking of the Dopamine Transporter. J Neurosci 35:12845–12858. https://doi.org/10.1523/JNEUROSCI.1391-15.2015
8. Bolam JP, Pissadaki EK (2012) Living on the edge with too many mouths to feed: Why dopamine neurons die. Mov Disord 27:1478–1483. https://doi.org/10.1002/mds.25135
9. Cragg SJ, Nicholson C, Kume-Kick J, Tao L, Rice ME (2001) Dopamine-Mediated Volume Transmission in Midbrain Is Regulated by Distinct Extracellular Geometry and Uptake. J Neurophysiol 85:1761–1771. https://doi.org/10.1152/jn.2001.85.4.1761

10. Ford CP (2014) The role of D2-autoreceptors in regulating dopamine neuron activity and transmission. Neuroscience, The Ventral Tegmentum and Dopamine: A New Wave of Diversity 282, 13–22. https://doi.org/10.1016/j.neuroscience.2014.01.025
11. Gantz SC, Robinson BG, Buck DC, Bunzow JR, Neve RL, Williams JT, Neve KA (2015) Distinct regulation of dopamine D2S and D2L autoreceptor signaling by calcium. eLife 4:e09358. https://doi.org/10.7554/eLife.09358
12. Gentet LJ, Williams SR (2007) Dopamine Gates Action Potential Backpropagation in Midbrain Dopaminergic Neurons. J Neurosci 27:1892–1901. https://doi.org/10.1523/JNEUROSCI.5234-06.2007
13. Giguère N, Delignat-Lavaud B, Herborg F, Voisin A, Li Y, Jacquemet V, Anand-Srivastava M, Gether U, Giros B, Trudeau L-É (2019) Increased vulnerability of nigral dopamine neurons after expansion of their axonal arborization size through D2 dopamine receptor conditional knockout. PLOS Genet 15:e1008352. https://doi.org/10.1371/journal.pgen.1008352
14. González-Cabrera C, Meza R, Ulloa L, Merino-Sepúlveda P, Luco V, Sanhueza A, Oñate-Ponce A, Bolam JP, Henny P (2017) Characterization of the axon initial segment of mice substantia nigra dopaminergic neurons. J Comp Neurol 525:3529–3542. https://doi.org/10.1002/cne.24288
15. Grace AA (2016) Dysregulation of the dopamine system in the pathophysiology of schizophrenia and depression. Nat Rev Neurosci 17:524–532. https://doi.org/10.1038/nrn.2016.57
16. Grace AA, Bunney BS (1983) Intracellular and extracellular electrophysiology of nigral dopaminergic neurons—1. Identification characterization Neuroscience 10:301–315. https://doi.org/10.1016/0306-4522(83)90135-5
17. Groves PM, Linder JC (1983) Dendro-dendritic synapses in substantia nigra: Descriptions based on analysis of serial sections. Exp Brain Res 49:209–217. https://doi.org/10.1007/BF00238581
18. Guthrie DA, Klein Herenbrink C, Lycas MD, Ku T, Bonifazi A, DeVree BT, Mathiasen S, Javitch JA, Grimm JB, Lavis L, Gether U, Newman AH (2020) Novel Fluorescent Ligands Enable Single-Molecule Localization Microscopy of the Dopamine Transporter. ACS Chem Neurosci 11:3288–3300. https://doi.org/10.1021/acschemneuro.0c00397
19. Guzman JN, Sanchez-Padilla J, Wokosin D, Kondapalli J, Ilijic E, Schumacker PT, Surmeier DJ (2010) Oxidant stress evoked by pacemaking in dopaminergic neurons is attenuated by DJ-1. Nature 468:696–700. https://doi.org/10.1038/nature09536
20. Hirsch E, Graybiel AM, Agid YA (1988) Melanized dopaminergic neurons are differentially susceptible to degeneration in Parkinson's disease. Nature 334:345–348. https://doi.org/10.1038/334345a0
21. Hrabetova S, Cognet L, Rusakov DA, Nägerl UV (2018) Unveiling the Extracellular Space of the Brain: From Super-resolved Microstructure to In Vivo Function. J Neurosci 38:9355–9363. https://doi.org/10.1523/JNEUROSCI.1664-18.2018
22. Koob GF, Volkow ND (2016) Neurobiology of addiction: a neurocircuitry analysis. Lancet Psychiatry 3:760–773. https://doi.org/10.1016/S2215-0366(16)00104-8

23. Pacelli C, Giguère N, Bourque M-J, Lévesque M, Slack RS, Trudeau L-É (2015) Elevated Mitochondrial Bioenergetics and Axonal Arborization Size Are Key Contributors to the Vulnerability of Dopamine Neurons. Curr Biol 25:2349–2360. https://doi.org/10.1016/j.cub.2015.07.050
24. Pontieri FE, Tanda G, Chiara GD (1995) Intravenous cocaine, morphine, and amphetamine preferentially increase extracellular dopamine in the “shell” as compared with the “core” of the rat nucleus accumbens. Proc. Natl. Acad. Sci. 92, 12304–12308. https://doi.org/10.1073/pnas.92.26.12304
25. Robinson BG, Bunzow JR, Grimm JB, Lavis LD, Dudman JT, Brown J, Neve KA, Williams JT (2017) Desensitized D2 autoreceptors are resistant to trafficking. Sci Rep 7:1–14. https://doi.org/10.1038/s41598-017-04728-z
26. Schneider Gasser EM, Straub CJ, Panzanelli P, Weinmann O, Sassoè-Pognetto M, Fritschy J-M (2006) Immunofluorescence in brain sections: simultaneous detection of presynaptic and postsynaptic proteins in identified neurons. Nat Protoc 1:1887–1897. https://doi.org/10.1038/nprot.2006.265
27. Sesack SR, Aoki C, Pickel VM (1994) Ultrastructural localization of D2 receptor-like immunoreactivity in midbrain dopamine neurons and their striatal targets. J Neurosci 14:88–106. https://doi.org/10.1523/JNEUROSCI.14-01-00088.1994
28. Surmeier DJ, Obeso JA, Halliday GM (2017) Selective neuronal vulnerability in Parkinson disease. Nat Rev Neurosci 18:101–113. https://doi.org/10.1038/nrn.2016.178
29. Touhara KK, MacKinnon R (2018) Molecular basis of signaling specificity between GIRK channels and GPCRs. eLife 7:e42908. https://doi.org/10.7554/eLife.42908
30. Tripp G, Wickens JR (2009) Neurobiology of ADHD. Neuropharmacology, Attention deficit hyperactivity disorder (ADHD): Improved understanding and novel drug treatment 57, 579–589. https://doi.org/10.1016/j.neuropharm.2009.07.026
31. Uchigashima M, Ohtsuka T, Kobayashi K, Watanabe M (2016) Dopamine synapse is a neuroligin-2–mediated contact between dopaminergic presynaptic and GABAergic postsynaptic structures. Proc. Natl. Acad. Sci. 113, 4206–4211. https://doi.org/10.1073/pnas.1514074113
32. Weijden MCM, van der, Rodriguez-Contreras D, Delnooz CCS, Robinson BG, Condon AF, Kielhold ML, Stormezand GN, Ma KY, Dufke C, Williams JT, Neve KA, Tijssen MAJ, Verbeek DS (2020) A Gain-of-Function Variant in Dopamine D2 Receptor and Progressive Chorea and Dystonia Phenotype. Mov. Disord. n/a. https://doi.org/10.1002/mds.28385
33. Yung KKL, Bolam JP, Smith AD, Hersch SM, Ciliax BJ, Levey AI (1995) Immunocytochemical localization of D1 and D2 dopamine receptors in the basal ganglia of the rat: Light and electron microscopy. Neuroscience 65:709–730. https://doi.org/10.1016/0306-4522(94)00536-E

Tables

Table 1. Spatial distribution of SEP-D2Rs on SNc dendrites.

Mean intensity +α-GFP (AFU)	Mean intensity -α-GFP (AFU)	Total # of detected puncta (/μm^3)	Fraction associated with TH	TH-associated desity (/μm^2)	Nearest neighbor (μm)
3,669 ± 319	1,366 ± 101	0.087 ± 0.020	0.446 ± 0.031	0.180 ± 0.023	1.326 ± 0.091

Figures

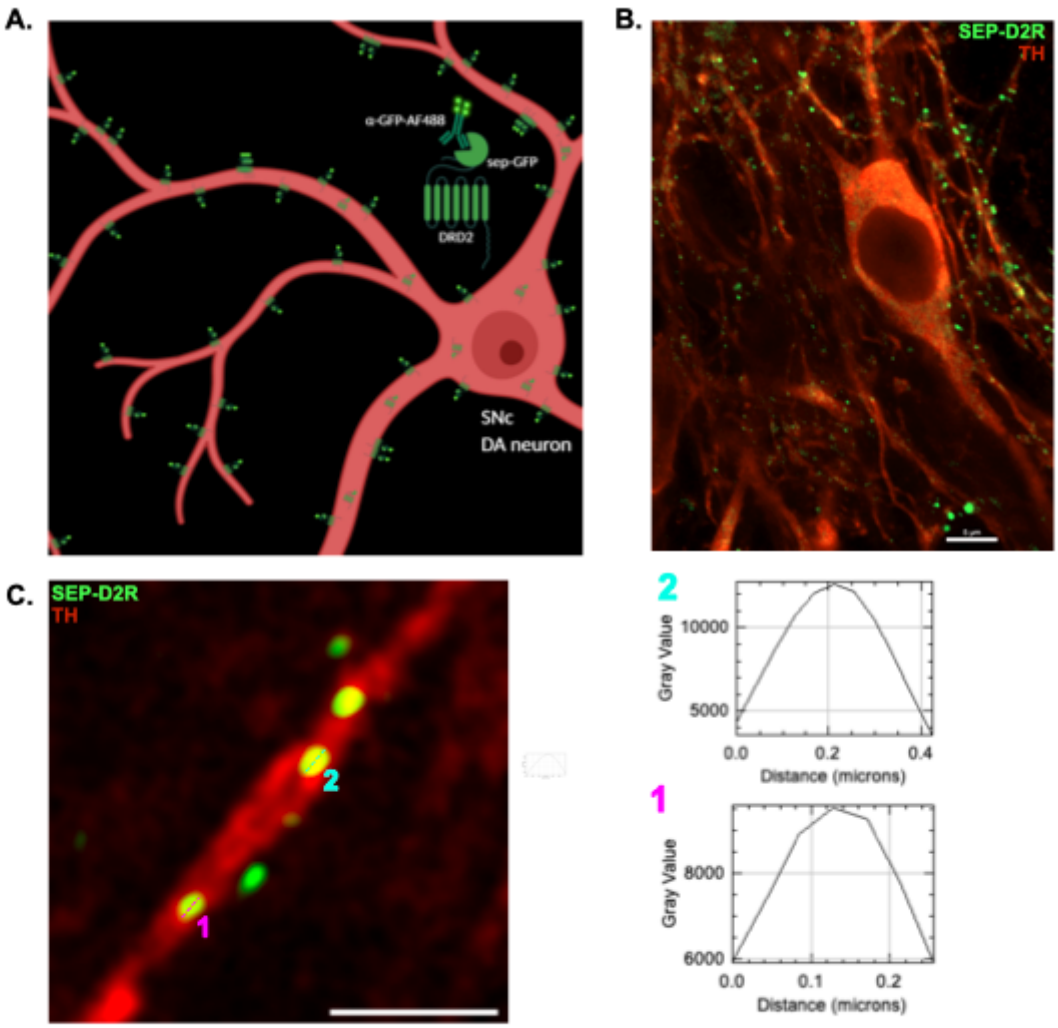

Figure 1

Visualizing SEP-D2R in SNc dopamine neurons A. Schematic of the live labeling approach used to amplify the signal of SEP-D2Rs on the cell surface. Not pictured are SEP-D2Rs expressed in non-

dopaminergic cells, identified by a lack of association with TH(+) staining. B. Single optical plane of an Airyscan image showing labeled SEP-D2Rs (green) on the soma and dendritic processes of SNc dopamine neurons labeled for TH (red). C. Representative image of individual SEP-D2R puncta and the spatial distribution of intensity (gray values, AFUs) along the central axis of annotated puncta in the X/Y plane. Distance is measured at a single plane through the central point of the punctum in z. Scale = 2.5 µm.

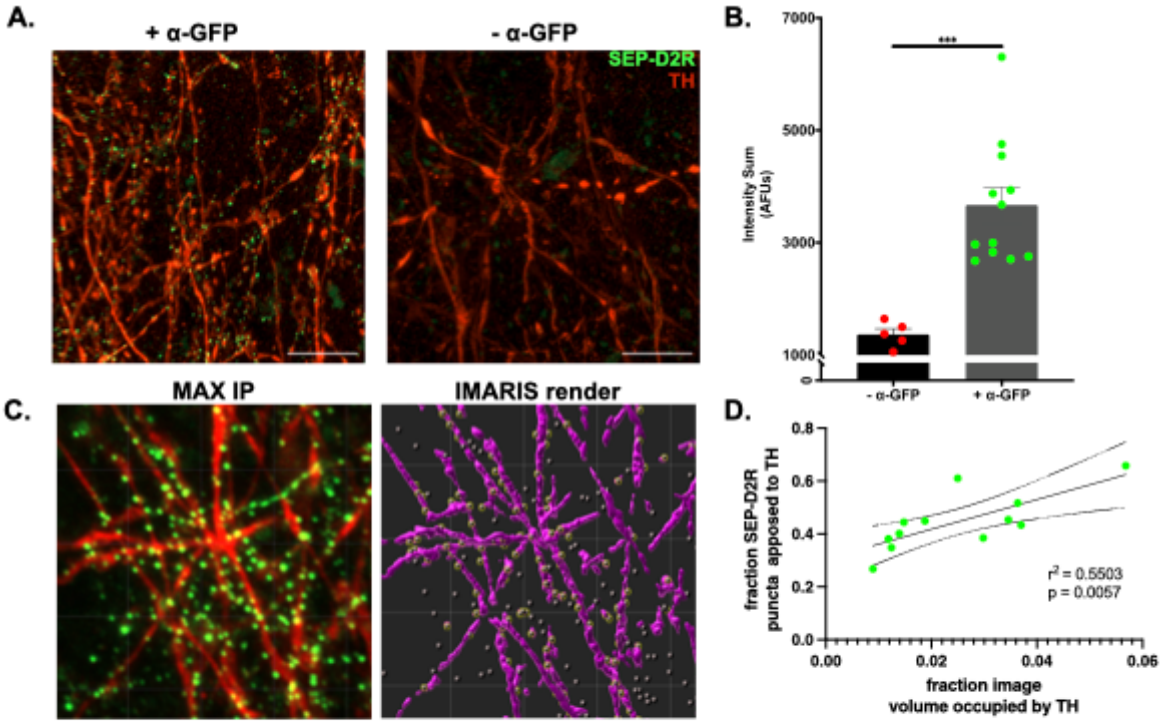

Figure 2

3D reconstruction of labeled SEP-D2Rs on TH(+) dendritic processes A. Maximum intensity projections of Airyscan z-stacks with identical dimensions displaying the intensity difference between antibody-labeled (+ α-GFP, left) SEP-D2Rs and the contribution of intrinsic SEP-D2R fluorescence in a slice from the same animal not exposed to α-GFP-AF488 (- α-GFP, right). Scale – 10 µm B. Raw intensity data of the brightest 40% of detected puncta in 3D reconstructions of tissue with (+) or without (-) α-GFP-AF488 (***, $p < .001$, unpaired t-test). C. 2D projection of reconstructed dendrites (left) and the rendered TH(+) surface and identified SEP-D2R puncta that either are associated with the surface (yellow circles) or are not (unmarked), i.e. are located >250nm from the TH(+) surface. D. Dependency of TH association of puncta on total TH surface volume imaged. (n = 12 images from 4 animals)

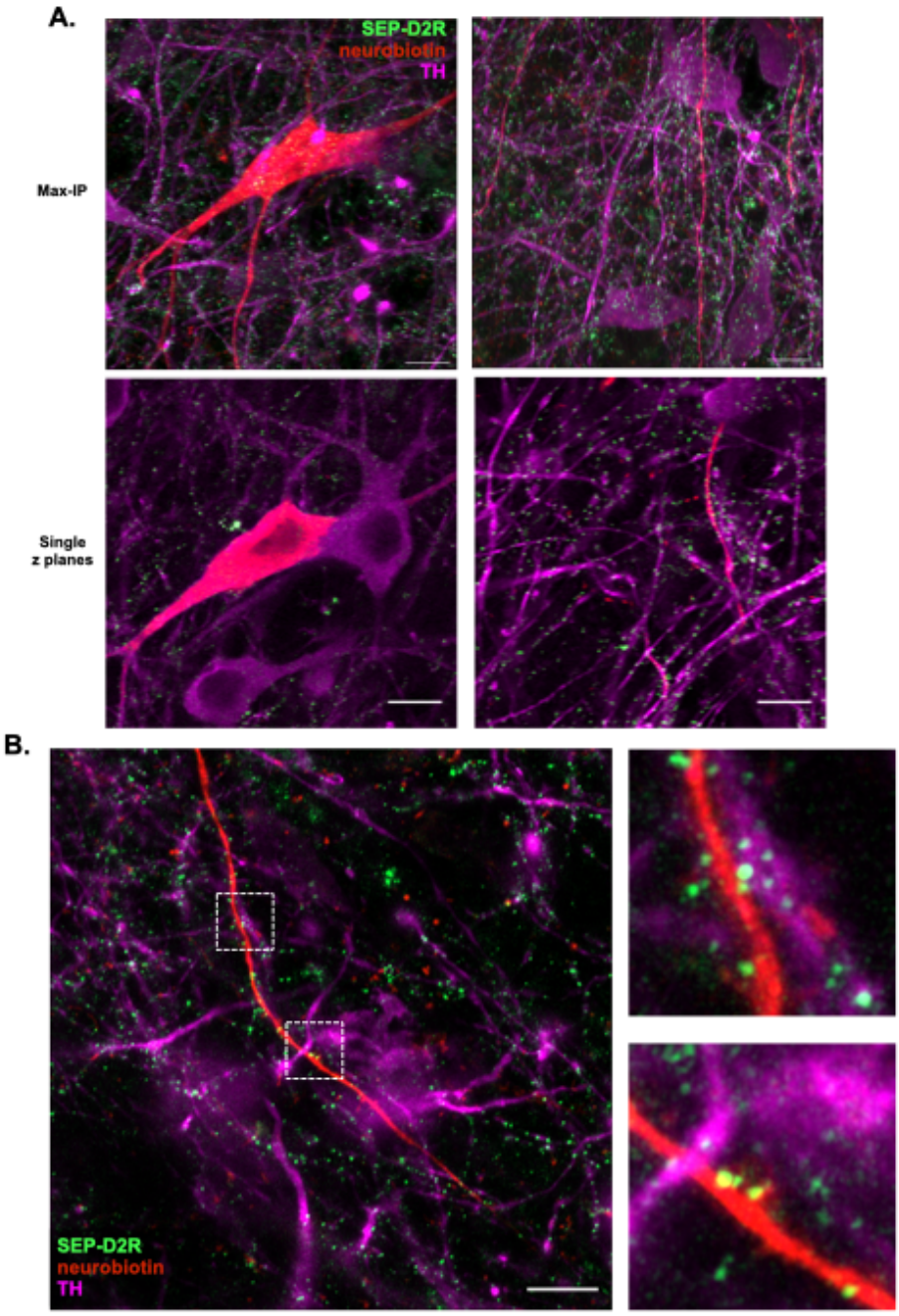

Figure 3

SEP-D2Rs are present at dendro-dendritic intersections distal from the cell body A. Maximum intensity projections (top) and single optical section (middle, bottom) showing the soma and proximal dendrites of a single Neurobiotin-filled SNc dopamine neuron. Receptor puncta can be seen in proximity to TH(+) processes (magenta), possibly constituting sites of dendro-dendritic communication. B. Dendritic SEP-D2Rs on a second labeled cell >100 µm from soma exiting from the SNc. Distal SEP-GFP-D2R puncta can

be seen at or near dendro-dendritic crossings, possibly constituting sites of dendro-dendritic communication.